Boundary Observer Design for Hyperbolic PDE-ODE Cascade Systems ⋆

Agus Hasan [a], Ole Morten Aamo [a], and Miroslav Krstic [b]

[a] *Department of Engineering Cybernetics*
Norwegian University of Science and Technology
Trondheim, Norway

[b] *Department of Mechanical and Aerospace Engineering*
University of California San Diego
California, USA

Abstract

The paper presents an observer design for a class of hyperbolic PDE-ODE cascade systems with a boundary measurement. The cascade systems consist of coupled PDEs, featuring one rightward and one leftward convecting first-order transport PDEs, and a set of ODEs, which enter the PDEs through the left boundary of the systems. The design, which is based on the Volterra integral transformation, relies only on a single sensor at the right boundary of the system. The observer consists of a copy of the plant plus output injection terms both in the PDEs and the ODEs. The observer is constructed in a collocated setup, which means both sensing and actuation are located at the same boundary. The observer gains are computed analytically by solving Goursat-type PDEs in terms of Bessel function of the first kind. The observer design is tested against a field scale flow-loop test experiment in Stavanger by Statoil Oil Company. The results show that the observer converges to the actual values and that the design can be used as a process monitoring tool in oil well drilling.

Key words: Distributed parameter systems, Cascade systems, Nonlinear systems, Observer design, State monitoring.

1 Introduction

1.1 Problem Statement

We consider a boundary observer design for a class of semilinear hyperbolic PDE-ODE cascade systems which can be transformed into the following form:

$$\mathbf{w}_t(x,t) = \mathbf{\Sigma}(x)\mathbf{w}_x(x,t) + \mathbf{\Omega}(x)\mathbf{w}(x,t) + \mathbf{f}(\mathbf{w}(x,t),x) \quad (1)$$
$$w_1(0,t) = qw_2(0,t) + \mathbf{C}\mathbf{X}(t) \quad (2)$$
$$w_2(1,t) = U(t) \quad (3)$$
$$\dot{\mathbf{X}}(t) = \mathbf{A}\mathbf{X}(t) \quad (4)$$

where $\mathbf{w} = [w_1\ w_2]^\intercal$ and $\mathbf{w} : [0,1] \times [0,\infty) \to \mathbb{R}^2$.

⋆ Financial support from Statoil ASA and the Norwegian Research Council (NFR project 210432/E30 Intelligent Drilling) is gratefully acknowledged.

Email addresses: agusisma@itk.ntnu.no (Agus Hasan), ole.morten.aamo@itk.ntnu.no (Ole Morten Aamo), krstic@ucsd.edu (Miroslav Krstic).

The matrices $\mathbf{\Sigma}(x)$ and $\mathbf{\Omega}(x)$ are given by:

$$\mathbf{\Sigma}(x) = \begin{pmatrix} -\epsilon_1(x) & 0 \\ 0 & \epsilon_2(x) \end{pmatrix}, \quad \mathbf{\Omega}(x) = \begin{pmatrix} 0 & \omega_1(x) \\ \omega_2(x) & 0 \end{pmatrix} \quad (5)$$

where $\epsilon_1(x),\ \epsilon_2(x) > 0$. The subscripts x and t denote partial derivatives with respect to x and t, respectively. The constant $q \neq 0$ and $U(t)$ is the control input. $\mathbf{X}(t)$ is an $n-$dimensional vector, $\mathbf{A}$ is an $n \times n$ matrix and $\mathbf{C}$ is an $1 \times n$ matrix. The function $\mathbf{f} : \mathbb{R}^2 \times [0,1] \to \mathbb{R}^2$ constitutes nonlinear terms. The objective of this paper is to design an observer for the cascade system (1)-(4) with only one boundary measurement at $x = 1$, i.e.,

$$y(t) = w_1(1,t). \quad (6)$$

This state observer problem was solved for the linear case without disturbance ($\mathbf{f} = 0$, $\mathbf{A} = 0$, and $\mathbf{C} = 0$) in [1] and for the linear case with disturbance in [2]. In [3], the state feedback stabilization problem was solved for the quasilinear systems (without disturbance). The controllability of the quasilinear systems with nonlinear

source have been studied in, e.g., [4].

The following assumptions are used in this paper:
Assumption 1 *The first derivatives of the entries in* $\mathbf{\Sigma}$ *are continuously differentiable, i.e.,* $\epsilon_1, \epsilon_2 \in \mathbb{C}^1([0,1])$*, while the entries in* $\mathbf{\Omega}$ *are continuous, i.e.,* $\omega_1, \omega_2 \in \mathbb{C}([0,1])$.
Assumption 2 *The function* $\mathbf{f}$ *is twice continuously differentiable with respect to* $\mathbf{w}$*. Furthermore,* $\mathbf{f}(0,x) = 0$ *and* $\frac{\mathrm{d}\mathbf{f}}{\mathrm{d}x}(0,x) = 0$.
Assumption 3 *The pair* $(\mathbf{A}, \mathbf{C})$ *is observable.*
Assumption 4 *The control law* U *is continuous, i.e.,* $U \in \mathbb{C}([0,\infty))$.

1.2 Motivation and Previous Works

Physical systems which can be modeled and transformed into the first-order hyperbolic PDE-ODE cascade systems (1)-(4) have attracted considerable attention in research communities because these systems can be used to model various processes such as road traffic [5], gas flow pipeline [6], and flow of fluids in transmission lines [7,8] and in open channels [9]. A typical problem is to estimate the states and the parameters of the systems using a limited number of measurements. In many cases, the only reliable measurement is located at the boundary. These estimated states and parameters are in turn used in a feedback control algorithm that automates the control input to maintain a desired state trajectory. Observer design for PDE-ODE cascade systems has been studied for many types of coupling such as an ODE and a diffusion PDE [10–12], an ODE and a hyperbolic PDE [13–15], and an ODE and a wave PDE [16,17].

The results in this paper employ the backstepping method, and in particular build on the results of [1,3,2]. The backstepping method has been successfully used as control and state estimation designs for many PDEs such as the parabolic-type equation [18,19], the Ginzburg-Landau equation [20], and the Schrodinger equation [21]. The idea is to use a Volterra integral transformation to transform the original system into a target system [22]. The stability of the target system is usually known beforehand. For some cases, the gains for both the controller and the observer, can be computed analytically in terms of the Bessel function [23] or the Marcum Q-function [24].

The applicability of the results obtained in the present paper are demonstrated on a problem from the oil and gas industry in Section 4. Backstepping has found several applications in oil and gas, including the gas coning problem [25,26], flow in porous media [27], slugging control [28], the lost circulation and kick problem [29–31], and the heave problem [32,33].

1.3 Contribution of this Paper

The contribution of this paper is an observer design for a class of hyperbolic PDE-ODE cascade systems with a boundary measurement. We employ a composition of two transformations, one Volterra-based backstepping transformation of the PDE observer state, and one transformation of the transformed PDE observer state with a spatially scaled shift based on the ODE observer state. The observer consists of the plant plus output injection terms, where the gains are found explicitly in terms of Bessel functions of the first kind. The stability of the target system is studied using a Lyapunov functional. Two cases are considered, linear ($\mathbf{f} = 0$) and semilinear ($\mathbf{f} \neq 0$). In the linear case we show that the observer error system is globally exponentially stable in the $\mathbb{L}^2$-norm, while in the semilinear case we show the observer error system is locally exponentially stable in the $\mathbb{H}^2$-norm. The observer design is tested against a field scale flow-loop test experiment in Stavanger by Statoil Oil Company.

1.4 Organization of the Paper

The paper is organized as follows. Section 2 contains preliminary definitions and notations used throughout the paper. The observer designs for both linear and semilinear cases are presented in Section 3. In Section 4, a real case application of oil well drilling where we estimate the flow, the pressure, and the downhole rate under lost circulation is presented. Finally, Section 5 contains conclusions and recommendations.

2 Preliminary Definitions

For a vector $\boldsymbol{\gamma}(x) \in \mathbb{R}^2$ with components $\gamma_1(x)$ and $\gamma_2(x)$, we denote $|\boldsymbol{\gamma}(x)| = |\gamma_1(x)| + |\gamma_2(x)|$, and we define $\|\boldsymbol{\gamma}\|_\infty = \sup_{x\in[0,1]} |\boldsymbol{\gamma}(x)|$, $\|\boldsymbol{\gamma}\|_{\mathbb{L}^1} = \int_0^1 |\boldsymbol{\gamma}(\xi)|\,\mathrm{d}\xi$, and $\|\boldsymbol{\gamma}\|_{\mathbb{L}^2} = \left(\int_0^1 \boldsymbol{\gamma}(\xi)^\intercal \boldsymbol{\gamma}(\xi)\,\mathrm{d}\xi\right)^{1/2}$. Furthermore, we define the following norms:

$$\|\boldsymbol{\gamma}\|_{\mathbb{H}^1} = \left(\|\boldsymbol{\gamma}\|_{\mathbb{L}^2}^2 + \int_0^1 \boldsymbol{\gamma}_x(\xi)^\intercal \boldsymbol{\gamma}_x(\xi)\,\mathrm{d}\xi\right)^{1/2} \tag{7}$$

$$\|\boldsymbol{\gamma}\|_{\mathbb{H}^2} = \left(\|\boldsymbol{\gamma}\|_{\mathbb{H}^1}^2 + \int_0^1 \boldsymbol{\gamma}_{xx}(\xi)^\intercal \boldsymbol{\gamma}_{xx}(\xi)\,\mathrm{d}\xi\right)^{1/2}. \tag{8}$$

For a 2×2 matrix $\mathbf{D}$, we denote:

$$|\mathbf{D}| = \max\left\{|\mathbf{D}v|; v \in \mathbb{R}^2, |v| = 1\right\}. \tag{9}$$

For the kernel matrices $\mathbf{K}$, we denote:

$$\|\mathbf{K}\|_\infty = \sup_{(x,\xi)\in\mathscr{T}} |\mathbf{K}(x,\xi)|. \tag{10}$$

where $\mathscr{T} = \{(x,\xi) : 0 \le \xi \le x \le 1\}$. For $\boldsymbol{\gamma} \in \mathbb{H}^2([0,1])$ and positive constants c_1, c_2, c_3, c_4, c_5, and c_6, recall the following well-known inequalities [3]:

$$\|\boldsymbol{\gamma}\|_{\mathbb{L}^1} \le c_1\|\boldsymbol{\gamma}\|_{\mathbb{L}^2} \le c_2\|\boldsymbol{\gamma}\|_\infty \tag{11}$$
$$\|\boldsymbol{\gamma}\|_\infty \le c_3\left(\|\boldsymbol{\gamma}\|_{\mathbb{L}^2} + \|\boldsymbol{\gamma}_x\|_{\mathbb{L}^2}\right) \le c_4\|\boldsymbol{\gamma}\|_{\mathbb{H}^1} \tag{12}$$
$$\|\boldsymbol{\gamma}_x\|_\infty \le c_5\left(\|\boldsymbol{\gamma}_x\|_{\mathbb{L}^2} + \|\boldsymbol{\gamma}_{xx}\|_{\mathbb{L}^2}\right) \le c_6\|\boldsymbol{\gamma}\|_{\mathbb{H}^2}. \tag{13}$$

3 Observer Design

We consider first the linear case, $\mathbf{f} = 0$. The semilinear design is found by utilizing the result from the linear design. We assume that we can measure $w_1(x,t)$ at $x = 1$, and design an observer to estimate both $\mathbf{w}$ and $\mathbf{X}$.

3.1 Linear System

We design the collocated observer as a copy of the plant plus output injection, that is

$$\hat{\mathbf{w}}_t = \boldsymbol{\Sigma}(x)\hat{\mathbf{w}}_x + \boldsymbol{\Omega}(x)\hat{\mathbf{w}} + \mathbf{p}(x)\left(w_1(1,t) - \hat{w}_1(1,t)\right) \tag{14}$$
$$\hat{w}_1(0,t) = q\hat{w}_2(0,t) + \mathbf{C}\hat{\mathbf{X}}(t) \tag{15}$$
$$\hat{w}_2(1,t) = U(t) \tag{16}$$
$$\dot{\hat{\mathbf{X}}}(t) = \mathbf{A}\hat{\mathbf{X}}(t) + e^{\mathbf{A}d}\mathbf{L}\left(w_1(1,t) - \hat{w}_1(1,t)\right). \tag{17}$$

where $d = \int_0^1 \frac{\mathrm{d}\chi}{\epsilon_1(\chi)}$. Defining error functions as $\tilde{\mathbf{w}} = \mathbf{w} - \hat{\mathbf{w}}$ and $\tilde{\mathbf{X}} = \mathbf{X} - \hat{\mathbf{X}}$, the error dynamics is given by

$$\tilde{\mathbf{w}}_t = \boldsymbol{\Sigma}(x)\tilde{\mathbf{w}}_x + \boldsymbol{\Omega}(x)\tilde{\mathbf{w}} - \mathbf{p}(x)\tilde{w}_1(1,t) \tag{18}$$
$$\tilde{w}_1(0,t) = q\tilde{w}_2(0,t) + \mathbf{C}\tilde{\mathbf{X}}(t) \tag{19}$$
$$\tilde{w}_2(1,t) = 0 \tag{20}$$
$$\dot{\tilde{\mathbf{X}}}(t) = \mathbf{A}\tilde{\mathbf{X}}(t) - e^{\mathbf{A}d}\mathbf{L}\tilde{w}_1(1,t) \tag{21}$$

where the observer gains $\mathbf{p}(x) = [p_1(x) \quad p_2(x)]^\intercal$ and $\mathbf{L}$ will be determined later. Define a new variable $\tilde{\boldsymbol{\gamma}} = [\tilde{\gamma}_1 \ \tilde{\gamma}_2]^\intercal$ using the following transformation:

$$\tilde{\mathbf{w}}(x,t) = \tilde{\boldsymbol{\gamma}}(x,t) - \int_x^1 \mathbf{P}(x,\xi)\tilde{\boldsymbol{\gamma}}(\xi,t)\,\mathrm{d}\xi \tag{22}$$

where

$$\mathbf{P}(x,\xi) = \begin{pmatrix} P^{uu}(x,\xi) & P^{uv}(x,\xi) \\ P^{vu}(x,\xi) & P^{vv}(x,\xi) \end{pmatrix} \tag{23}$$

is the solution to the first-order hyperbolic PDE

$$\epsilon_1(x)P^{uu}_x + \epsilon_1(\xi)P^{uu}_\xi = -\epsilon_1'(\xi)P^{uu} + \omega_1(x)P^{vu} \tag{24}$$
$$\epsilon_1(x)P^{uv}_x - \epsilon_2(\xi)P^{uv}_\xi = \epsilon_2'(\xi)P^{uv} + \omega_1(x)P^{vv} \tag{25}$$
$$\epsilon_2(x)P^{vu}_x - \epsilon_1(\xi)P^{vu}_\xi = \epsilon_1'(\xi)P^{vu} - \omega_2(x)P^{uu} \tag{26}$$
$$\epsilon_2(x)P^{vv}_x + \epsilon_2(\xi)P^{vv}_\xi = -\epsilon_2'(\xi)P^{vv} - \omega_2(x)P^{uv} \tag{27}$$

with boundary conditions

$$P^{uu}(0,\xi) = qP^{vu}(0,\xi) \tag{28}$$
$$P^{uv}(x,x) = \frac{\omega_1(x)}{\epsilon_1(x) + \epsilon_2(x)} \tag{29}$$
$$P^{vu}(x,x) = -\frac{\omega_2(x)}{\epsilon_1(x) + \epsilon_2(x)} \tag{30}$$
$$P^{vv}(0,\xi) = \frac{1}{q}P^{uv}(0,\xi) \tag{31}$$

on the triangular domain $\mathscr{T}$. It was shown in [1] that there is a unique solution of the kernel system (24)-(31) which is in $\mathbb{C}(\mathscr{T})$ and that (22) has an inverse. Remark that, due to (31), the method presented in this paper is not valid for $q = 0$. The method can be adapted to accommodate zero values of q by setting a slightly different target system (see section 3.5 in [3]).

The transformation (22) is used to transform (18)-(21) into a new cascade system (Lemma 1) where the finite time stability of the new cascade system is investigated using Lyapunov functionals (Lemma 2).

Lemma 1 *Let the elements of the observer gain* $\mathbf{p}(x)$ *in* (18) *be given by*

$$p_1(x) = \mathbf{C}e^{\mathbf{A}h(x)}\mathbf{L} - \epsilon_1(1)P^{uu}(x,1) - \int_x^1 P^{uu}(x,\xi)\mathbf{C}e^{\mathbf{A}h(\xi)}\mathbf{L}\,\mathrm{d}\xi \tag{32}$$
$$p_2(x) = -\epsilon_1(1)P^{vu}(x,1) - \int_x^1 P^{vu}(x,\xi)\mathbf{C}e^{\mathbf{A}h(\xi)}\mathbf{L}\,\mathrm{d}\xi \tag{33}$$

where P^{uu} *and* P^{vu} *are the solutions to* (24), (26), (28), *and* (30), *and*

$$h(x) = \int_x^1 \frac{\mathrm{d}\chi}{\epsilon_1(\chi)}. \tag{34}$$

Then, the transformation (22) *maps the system*

$$\tilde{\boldsymbol{\gamma}}_t = \boldsymbol{\Sigma}(x)\tilde{\boldsymbol{\gamma}}_x + \bar{\mathbf{p}}(x)\tilde{\gamma}_1(1,t) \tag{35}$$
$$\tilde{\gamma}_1(0,t) = q\tilde{\gamma}_2(0,t) + \mathbf{C}\tilde{\mathbf{X}}(t) \tag{36}$$
$$\tilde{\gamma}_2(1,t) = 0 \tag{37}$$
$$\dot{\tilde{\mathbf{X}}}(t) = \mathbf{A}\tilde{\mathbf{X}}(t) - e^{\mathbf{A}d}\mathbf{L}\tilde{\gamma}_1(1,t) \tag{38}$$

into (18)-(21) *with* $\bar{\mathbf{p}}(x) = [-\mathbf{C}e^{\mathbf{A}h(x)}\mathbf{L}\ 0]^\intercal$.

Proof *From* (22) *we have:*

$$\begin{aligned}\tilde{w}_{1t}(x,t) &= \tilde{\gamma}_{1t}(x,t) - \int_x^1 P^{uu}(x,\xi)\tilde{\gamma}_{1t}(\xi,t)\,\mathrm{d}\xi \\ &\quad - \int_x^1 P^{uv}(x,\xi)\tilde{\gamma}_{2t}(\xi,t)\,\mathrm{d}\xi \qquad (39)\\ \tilde{w}_{1x}(x,t) &= \tilde{\gamma}_{1x}(x,t) - \int_x^1 P^{uu}_x(x,\xi)\tilde{\gamma}_1(\xi,t)\,\mathrm{d}\xi \\ &\quad + P^{uu}(x,x)\tilde{\gamma}_1(x,t) \\ &\quad - \int_x^1 P^{uv}_x(x,\xi)\tilde{\gamma}_2(\xi,t)\,\mathrm{d}\xi \\ &\quad + P^{uv}(x,x)\tilde{\gamma}_2(x,t). \qquad (40)\end{aligned}$$

Plugging (35) *into* (39)*, yields:*

$$\begin{aligned}\tilde{w}_{1t}(x,t) &= -\epsilon_1(x)\tilde{\gamma}_{1x}(x,t) - \mathbf{C}e^{\mathbf{A}h(x)}\mathbf{L}\tilde{\gamma}_1(1,t) \\ &\quad + \int_x^1 P^{uu}(x,\xi)\mathbf{C}e^{\mathbf{A}h(\xi)}\mathbf{L}\tilde{\gamma}_1(1,t)\,\mathrm{d}\xi \\ &\quad + \int_x^1 \epsilon_1(\xi)P^{uu}(x,\xi)\tilde{\gamma}_{1x}(\xi,t)\,\mathrm{d}\xi \\ &\quad - \int_x^1 \epsilon_2(\xi)P^{uv}(x,\xi)\tilde{\gamma}_{2x}(\xi,t)\,\mathrm{d}\xi. \qquad (41)\end{aligned}$$

Integration by parts the last two terms of the right hand side, yields:

$$\begin{aligned}&\int_x^1 \epsilon_1(\xi)P^{uu}(x,\xi)\tilde{\gamma}_{1x}(\xi,t)\,\mathrm{d}\xi = \\ &\epsilon_1(1)P^{uu}(x,1)\tilde{\gamma}_1(1,t) - \epsilon_1(x)P^{uu}(x,x)\tilde{\gamma}_1(x,t) \\ &- \int_x^1 \left(\epsilon_1(\xi)P^{uu}_\xi(x,\xi) + \epsilon_1'(\xi)P^{uu}(x,\xi)\right)\tilde{\gamma}_1(\xi,t)\,\mathrm{d}\xi \qquad (42)\\ &- \int_x^1 \epsilon_2(\xi)P^{uv}(x,\xi)\tilde{\gamma}_{2x}(\xi,t)\,\mathrm{d}\xi = \\ &\epsilon_2(x)P^{uv}(x,x)\tilde{\gamma}_2(x,t) \\ &+ \int_x^1 \left(\epsilon_2(\xi)P^{uv}_\xi(x,\xi) + \epsilon_2'(\xi)P^{uv}(x,\xi)\right)\tilde{\gamma}_2(\xi,t)\,\mathrm{d}\xi. \qquad (43)\end{aligned}$$

Substituting those equations into (41)*, yields:*

$$\begin{aligned}&\tilde{w}_{1t}(x,t) = \\ &-\epsilon_1(x)\tilde{\gamma}_{1x}(x,t) - p_1(x)\tilde{\gamma}_1(1,t) \\ &-\epsilon_1(x)P^{uu}(x,x)\tilde{\gamma}_1(x,t) + \epsilon_2(x)P^{uv}(x,x)\tilde{\gamma}_2(x,t) \\ &- \int_x^1 \left(\epsilon_1(\xi)P^{uu}_\xi(x,\xi) + \epsilon_1'(\xi)P^{uu}(x,\xi)\right)\tilde{\gamma}_1(\xi,t)\,\mathrm{d}\xi \\ &+ \int_x^1 \left(\epsilon_2(\xi)P^{uv}_\xi(x,\xi) + \epsilon_2'(\xi)P^{uv}(x,\xi)\right)\tilde{\gamma}_2(\xi,t)\,\mathrm{d}\xi. \qquad (44)\end{aligned}$$

Plugging (40) *into the above equation, yields:*

$$\begin{aligned}&\tilde{w}_{1t}(x,t) = \\ &-\epsilon_1(x)\tilde{w}_{1x}(x,t) - p_1(x)\tilde{\gamma}_1(1,t) \\ &+ \left(\epsilon_1(x) + \epsilon_2(x)\right)P^{uv}(x,x)\tilde{\gamma}_2(x,t) \\ &- \int_x^1 \left(\epsilon_1(x)P^{uu}_x(x,\xi) + \epsilon_1(\xi)P^{uu}_\xi(x,\xi)\right. \\ &\left.+\epsilon_1'(\xi)P^{uu}(x,\xi)\right)\tilde{\gamma}_1(\xi,t)\,\mathrm{d}\xi \\ &- \int_x^1 \left(\epsilon_1(x)P^{uv}_x(x,\xi) - \epsilon_2(\xi)P^{uv}_\xi(x,\xi)\right. \\ &\left.-\epsilon_2'(\xi)P^{uv}(x,\xi)\right)\tilde{\gamma}_2(\xi,t)\,\mathrm{d}\xi. \qquad (45)\end{aligned}$$

Substituting (22)*,* (24)*,* (25)*, and* (29)*, we obtain the first entry of* (18)*. Applying the same procedure we can obtain the second entry of* (18)*. Next, evaluating* (22) *at* $x = 0$*, yields:*

$$\begin{aligned}\tilde{w}_1(0,t) &= \tilde{\gamma}_1(0,t) - \int_0^1 P^{uu}(0,\xi)\tilde{\gamma}_1(\xi,t)\,\mathrm{d}\xi \\ &\quad - \int_0^1 P^{uv}(0,\xi)\tilde{\gamma}_2(\xi,t)\,\mathrm{d}\xi \qquad (46)\\ \tilde{\gamma}_2(0,t) &= \tilde{w}_2(0,t) + \int_0^1 P^{vu}(0,\xi)\tilde{\gamma}_1(\xi,t)\,\mathrm{d}\xi \\ &\quad + \int_0^1 P^{vv}(0,\xi)\tilde{\gamma}_2(\xi,t)\,\mathrm{d}\xi \qquad (47)\end{aligned}$$

Plugging (28)*,* (31)*, and* (36) *into* (46)*, yields:*

$$\begin{aligned}\tilde{w}_1(0,t) &= q\tilde{\gamma}_2(0,t) + \mathbf{C}\tilde{\mathbf{X}}(t) - q\int_0^1 P^{vu}(0,\xi)\tilde{\gamma}_1(\xi,t)\,\mathrm{d}\xi \\ &\quad - q\int_0^1 P^{vv}(0,\xi)\tilde{\gamma}_2(\xi,t)\,\mathrm{d}\xi. \qquad (48)\end{aligned}$$

Plugging (47) *into the above equation, we obtain* (19)*.*

We can simplify the cascade (35)-(38) by defining a new variable $\tilde{\boldsymbol{\psi}} = [\tilde{\psi}_1\ \tilde{\psi}_2]^\intercal$ and using the transformation

$$\begin{pmatrix}\tilde{\psi}_1(x,t)\\ \tilde{\psi}_2(x,t)\end{pmatrix} = \begin{pmatrix}\tilde{\gamma}_1(x,t) - \mathbf{C}e^{\mathbf{A}(h(x)-d)}\tilde{\mathbf{X}}(t)\\ \tilde{\gamma}_2(x,t)\end{pmatrix}. \qquad (49)$$

Hence, (35)-(38) becomes

$$\begin{aligned}\tilde{\boldsymbol{\psi}}_t &= \boldsymbol{\Sigma}(x)\tilde{\boldsymbol{\psi}}_x \qquad (50)\\ \tilde{\psi}_1(0,t) &= q\tilde{\psi}_2(0,t) \qquad (51)\\ \tilde{\psi}_2(1,t) &= 0 \qquad (52)\\ \dot{\tilde{\mathbf{X}}}(t) &= e^{\mathbf{A}d}\left(\mathbf{A} - \mathbf{L}\mathbf{C}\right)e^{-\mathbf{A}d}\tilde{\mathbf{X}}(t) - e^{\mathbf{A}d}\mathbf{L}\tilde{\psi}_1(1,t). \qquad (53)\end{aligned}$$

The system (50)-(53) can be viewed as a cascade consisting of the part (50)-(52) and (53), where the former affects the latter through $\tilde{\psi}_1(1,t)$.

Lemma 2 *Consider system* (50)-(52) *with initial condition* $\tilde{\boldsymbol{\psi}}_0 \in \mathbb{L}^2([0,1])$. *Then, for every* $\lambda > 0$, *there exists* c *such that:*

$$\|\tilde{\boldsymbol{\psi}}(\cdot,t)\|_{\mathbb{L}^2} \leq ce^{-\lambda t}\|\tilde{\boldsymbol{\psi}}_0\|_{\mathbb{L}^2}. \tag{54}$$

Furthermore, the equilibrium $\tilde{\boldsymbol{\psi}} \equiv 0$ *is reached in finite time* $t = t_f$, *where* t_f *is given by:*

$$t_f = \int_0^1 \left(\frac{1}{\epsilon_1(\xi)} + \frac{1}{\epsilon_2(\xi)}\right) \mathrm{d}\xi. \tag{55}$$

Proof *Define a Lyapunov candidate function*

$$W_1(t) = \int_0^1 \tilde{\boldsymbol{\psi}}^{\intercal}(x,t)\mathbf{D}(x)\tilde{\boldsymbol{\psi}}(x,t)\,\mathrm{d}x \tag{56}$$

where

$$\mathbf{D}(x) = \begin{pmatrix} A\frac{e^{-\mu x}}{\epsilon_1(x)} & 0 \\ 0 & B\frac{e^{\mu x}}{\epsilon_2(x)} \end{pmatrix} \tag{57}$$

is a positive definite matrix for positive A *and* B. *Computing the first derivative of* (56) *with respect to time* t *along* (50) *and using integration by parts, yields:*

$$\begin{aligned}\dot{W}_1(t) = &-\int_0^1 \tilde{\boldsymbol{\psi}}^{\intercal}(x,t)\left(\mathbf{D}(x)\boldsymbol{\Sigma}(x)\right)_x\tilde{\boldsymbol{\psi}}(x,t)\,\mathrm{d}x \\ &+\left[\tilde{\boldsymbol{\psi}}^{\intercal}(x,t)\mathbf{D}(x)\boldsymbol{\Sigma}(x)\tilde{\boldsymbol{\psi}}(x,t)\right]_0^1.\end{aligned} \tag{58}$$

Using the boundary conditions (51) *and* (52), *we have:*

$$\begin{aligned}&\left[\tilde{\boldsymbol{\psi}}^{\intercal}(x,t)\mathbf{D}(x)\boldsymbol{\Sigma}(x)\tilde{\boldsymbol{\psi}}(x,t)\right]_0^1 = \\ &-A\tilde{\psi}_1(1,t)^2e^{-\mu} - \left(B - q^2A\right)\tilde{\psi}_2(0,t)^2.\end{aligned} \tag{59}$$

Choosing $B = q^2A + \lambda_2$, $A = \lambda_2 e^{\mu}$, *and* $\mu = \lambda_1\bar{\epsilon}$, *where* $\bar{\epsilon} = \max_{x\in[0,1]}\left\{\frac{1}{\epsilon_1(x)}, \frac{1}{\epsilon_2(x)}\right\}$ *and* $\lambda_1, \lambda_2 > 0$, *we have* $\left(\mathbf{D}(x)\boldsymbol{\Sigma}(x)\right)_x \geq \lambda_1\mathbf{D}(x)$. *Thus,* $\dot{W}_1(t) \leq -\lambda_1 W_1(t)$, *which shows that the equilibrium solution* $\tilde{\boldsymbol{\psi}}$ *is exponentially stable in the* $\mathbb{L}^2$*-norm. Furthermore, the system* (50)-(52) *is a cascade of two transport equations whose explicit solutions can be obtained. Defining* $\phi_1(x) = \int_0^x \frac{1}{\epsilon_1(\xi)}\,\mathrm{d}\xi$ *and* $\phi_2(x) = \int_0^x \frac{1}{\epsilon_2(\xi)}\,\mathrm{d}\xi$, *for initial condition* $\tilde{\psi}_{01}, \tilde{\psi}_{02} \in \mathbb{L}^2([0,1])$, *the solution is given by:*

$$\tilde{\psi}_1(x,t) = \begin{cases} \tilde{\psi}_{01}\left(\left(\phi_1^{-1}(\phi_1(x) - t)\right), & t \leq \phi_1(x) \\ q\tilde{\psi}_2\left(0, t - \phi_1(x)\right), & t \geq \phi_1(x) \end{cases} \tag{60}$$

$$\tilde{\psi}_2(x,t) = \begin{cases} \tilde{\psi}_{02}\left(\left(\phi_2^{-1}(\phi_2(x) + t)\right), & t \leq \phi_2(1) - \phi_2(x) \\ 0, & t \geq \phi_2(1) - \phi_2(x) \end{cases} \tag{61}$$

Hence, if we let $t_f = \phi_1(1) + \phi_2(1)$, *we get* $\tilde{\boldsymbol{\psi}} \equiv 0$. *This concludes the proof.*

Since $\tilde{\boldsymbol{\psi}}$ converges to zero in finite time, (53) becomes

$$\dot{\tilde{\mathbf{X}}}(t) = e^{\mathbf{A}d}\left(\mathbf{A} - \mathbf{LC}\right)e^{-\mathbf{A}d}\tilde{\mathbf{X}}(t). \tag{62}$$

Lemma 3 *Choose* $\mathbf{L}$ *such that* $(\mathbf{A} - \mathbf{LC})$ *is Hurwitz stable. Then* $\tilde{\mathbf{X}}$ *converges to zero exponentially.*

Utilizing Lemma 1, 2, and 3, we have the following result.

Theorem 1 *Let the components of the observer gain* $\mathbf{p}(x)$ *be given by* (32) *and* (33) *and choose* $\mathbf{L}$ *such that* $(\mathbf{A} - \mathbf{LC})$ *is Hurwitz stable. Then, for any initial condition* $\tilde{\mathbf{w}}_0 \in \mathbb{L}^2([0,1])$, *the error system* (18)-(21) *is exponentially stable in the norm*

$$\left|\tilde{\mathbf{X}}(t)\right|^2 + \|\tilde{\mathbf{w}}(\cdot,t)\|^2_{\mathbf{L}^2}. \tag{63}$$

Proof *Define*

$$W_2(t) = \tilde{\mathbf{X}}^{\intercal}(t)e^{-\mathbf{A}^{\intercal}d}\mathbf{S}e^{-\mathbf{A}d}\tilde{\mathbf{X}}(t) \tag{64}$$

where $\mathbf{S}$ *is a symmetric positive definite matrix, i.e.,* $\mathbf{S} = \mathbf{S}^{\intercal} > 0$, *that satisfies the Lyapunov equation*

$$\mathbf{S}\left(\mathbf{A} - \mathbf{LC}\right) + \left(\mathbf{A} - \mathbf{LC}\right)^{\intercal}\mathbf{S} = -\mathbf{T} \tag{65}$$

where $\mathbf{T}$ *is also a symmetric positive definite matrix, i.e.* $\mathbf{T} = \mathbf{T}^{\intercal} > 0$. *Define* $W(t) = W_1(t) + W_2(t)$. *Computing the first derivative of* W *with respect to* t, *yields*

$$\dot{W}(t) \leq -\lambda_1 W_1(t) - W_2(t) \leq -\Lambda W(t) \tag{66}$$

for some $\Lambda > 0$, *which shows that the cascade* (50)-(53) *is exponentially stable in the norm* $\left|\tilde{\mathbf{X}}(t)\right|^2 + \left\|\tilde{\boldsymbol{\psi}}(\cdot,t)\right\|^2_{\mathbf{L}^2}$. *Thus, from* (49), *the cascade* (35)-(38) *is exponentially stable in the norm* $\left|\tilde{\mathbf{X}}(t)\right|^2 + \|\tilde{\boldsymbol{\gamma}}(\cdot,t)\|^2_{\mathbf{L}^2}$. *The result now follows in view of* (22) *and its inverse, which both exist by the results in [1].*

3.2 Semilinear System

The observer for the semilinear system (1)-(4) is given by

$$\hat{\mathbf{w}}_t = \boldsymbol{\Sigma}(x)\hat{\mathbf{w}}_x + \boldsymbol{\Omega}(x)\hat{\mathbf{w}} + \mathbf{f}(\hat{\mathbf{w}}, x) + \mathbf{p}(x)\tilde{w}_1(1,t) \tag{67}$$

$$\hat{w}_1(0,t) = q\hat{w}_2(0,t) + \mathbf{C}\hat{\mathbf{X}}(t) \tag{68}$$

$$\hat{w}_2(1,t) = U(t) \tag{69}$$

$$\dot{\hat{\mathbf{X}}}(t) = \mathbf{A}\hat{\mathbf{X}}(t) + e^{\mathbf{A}d}\mathbf{L}\tilde{w}_1(1,t). \tag{70}$$

The error system is now

$$\tilde{\mathbf{w}}_t = \mathbf{\Sigma}(x)\tilde{\mathbf{w}}_x + \mathbf{\Omega}(x)\tilde{\mathbf{w}} + (\mathbf{f}(\tilde{\mathbf{w}}+\hat{\mathbf{w}}) - \mathbf{f}(\hat{\mathbf{w}})) - \mathbf{p}(x)\tilde{w}_1(1,t) \quad (71)$$

$$\tilde{w}_1(0,t) = q\tilde{w}_2(0,t) + \mathbf{C}\tilde{\mathbf{X}}(t) \quad (72)$$

$$\tilde{w}_2(1,t) = 0 \quad (73)$$

$$\dot{\tilde{\mathbf{X}}}(t) = \mathbf{A}\tilde{\mathbf{X}}(t) - e^{\mathbf{A}d}\mathbf{L}\tilde{w}_1(1,t). \quad (74)$$

To show the stability of the error system, we define the transformations

$$\hat{\mathbf{w}}(x,t) = \hat{\boldsymbol{\gamma}}(x,t) + \int_0^x \mathbf{R}(x,\xi)\hat{\boldsymbol{\gamma}}(\xi,t)\,\mathrm{d}\xi \quad (75)$$

$$\tilde{\boldsymbol{\gamma}}(x,t) = \tilde{\mathbf{w}}(x,t) + \int_x^1 \mathbf{Q}(x,\xi)\tilde{\mathbf{w}}(\xi,t)\,\mathrm{d}\xi \quad (76)$$

where the kernel matrices $\mathbf{R}$ and $\mathbf{Q}$ can be shown to exist [1]. In particular, the kernel matrix $\mathbf{R}$ is the solution of a system of equations analog to the kernel system (24)-(31). We proceed in this section as follows. The transformations (22), (75), and (76) are used to transform (71)-(74) into a new cascade system (Lemma 4) where the stability of the new cascade system is investigated using Lyapunov functionals (Lemma 5, 6, and 7).

Lemma 4 *The transformations* (22), (75), *and* (76) *map*

$$\tilde{\boldsymbol{\gamma}}_t = \mathbf{\Sigma}(x)\tilde{\boldsymbol{\gamma}}_x + \mathbf{F}[\tilde{\boldsymbol{\gamma}},\hat{\boldsymbol{\gamma}}] + \bar{\mathbf{p}}(x)\tilde{\gamma}_1(1,t) \quad (77)$$

$$\tilde{\gamma}_1(0,t) = q\tilde{\gamma}_2(0,t) + \mathbf{C}\tilde{\mathbf{X}}(t) \quad (78)$$

$$\tilde{\gamma}_2(1,t) = 0 \quad (79)$$

$$\dot{\tilde{\mathbf{X}}}(t) = \mathbf{A}\tilde{\mathbf{X}}(t) - e^{\mathbf{A}d}\mathbf{L}\tilde{\gamma}_1(1,t). \quad (80)$$

into (71)-(74) *with*

$$\mathbf{F}[\tilde{\boldsymbol{\gamma}},\hat{\boldsymbol{\gamma}}] = \mathcal{P}\left[\mathbf{f}\left(\mathcal{P}[\tilde{\boldsymbol{\gamma}}] + \mathcal{R}[\hat{\boldsymbol{\gamma}}]\right) - \mathbf{f}\left(\mathcal{R}[\hat{\boldsymbol{\gamma}}]\right)\right] \quad (81)$$

where

$$\mathcal{P}[\tilde{\boldsymbol{\gamma}}] = \tilde{\boldsymbol{\gamma}}(x,t) - \int_x^1 \mathbf{P}(x,\xi)\tilde{\boldsymbol{\gamma}}(\xi,t)\,\mathrm{d}\xi \quad (82)$$

$$\mathcal{R}[\hat{\boldsymbol{\gamma}}] = \hat{\boldsymbol{\gamma}}(x,t) + \int_0^x \mathbf{R}(x,\xi)\hat{\boldsymbol{\gamma}}(\xi,t)\,\mathrm{d}\xi \quad (83)$$

Proof *From Lemma 1, up to the linear part (*$\mathbf{F} = \mathbf{f} = 0$*), we show that the transformation* (22) *maps* (77)-(80) *into* (71)-(74)*. Applying the transformations* (75) *and* (76) *into* $\mathbf{F}$*, the nonlinear function which depends on* $\tilde{\boldsymbol{\gamma}}$ *and* $\hat{\boldsymbol{\gamma}}$ *is mapped into* $\mathbf{f}$ *which depends on* $\tilde{\mathbf{w}}$ *and* $\hat{\mathbf{w}}$*.*

The dependency of the nonlinear term $\mathbf{F}$ in (77) on $\hat{\boldsymbol{\gamma}}$ is a nontrivial problem when showing the convergence of the error function $\tilde{\boldsymbol{\gamma}}$. To overcome this issue, we employ the following assumption.

Assumption 5 *There exists* $M > 0$ *such that* $|\boldsymbol{\gamma}| \le M$ *uniformly in* $x \in [0,1]$ *and* $t \ge 0$*.*

Under this assumption, the nonlinear term becomes $\mathbf{F}[\tilde{\boldsymbol{\gamma}},\hat{\boldsymbol{\gamma}}] = \mathbf{F}[\tilde{\boldsymbol{\gamma}},\boldsymbol{\gamma}-\tilde{\boldsymbol{\gamma}}] = \mathbf{G}[\tilde{\boldsymbol{\gamma}}]$. Notice that the dependency on $\tilde{\boldsymbol{\gamma}}$ in $\mathbf{G}$ comes from (22), which along with the smoothness of $\mathbf{f}$ implies the bound

$$|\mathbf{G}(x,t)| \le C\left(|\tilde{\boldsymbol{\gamma}}|^2 + \|\tilde{\boldsymbol{\gamma}}\|_{\mathbb{L}^2}^2\right). \quad (84)$$

This bound is essential, gives rise to similar bounds for $\mathbf{G}_1$, $\mathbf{G}_2$, and $\mathbf{G}_3$ below, and is used to prove the main result of this section (see [3] for detail). Substituting (49) into (77)-(80), yield:

$$\tilde{\boldsymbol{\psi}}_t = \mathbf{\Sigma}(x)\tilde{\boldsymbol{\psi}}_x + \mathbf{G}_1[\tilde{\boldsymbol{\psi}},\tilde{\mathbf{X}}] \quad (85)$$

$$\tilde{\psi}_1(0,t) = q\tilde{\psi}_2(0,t) \quad (86)$$

$$\tilde{\psi}_2(1,t) = 0 \quad (87)$$

$$\dot{\tilde{\mathbf{X}}}(t) = e^{\mathbf{A}d}\left(\mathbf{A}-\mathbf{LC}\right)e^{-\mathbf{A}d}\tilde{\mathbf{X}}(t) - e^{\mathbf{A}d}\mathbf{L}\tilde{\psi}_1(1,t), \quad (88)$$

where

$$\mathbf{G}_1[\tilde{\boldsymbol{\psi}},\tilde{\mathbf{X}}] = \mathcal{P}\left[\mathbf{f}\left(\mathcal{O}[\tilde{\boldsymbol{\psi}}],\tilde{\mathbf{X}}\right) - \mathbf{f}\left(\mathcal{R}[\tilde{\boldsymbol{\psi}}],\tilde{\mathbf{X}}\right)\right], \quad (89)$$

and

$$\mathcal{O}[\tilde{\boldsymbol{\psi}}] = 2\tilde{\boldsymbol{\psi}}(x,t) - \int_x^1 \mathbf{P}(x,\xi)\tilde{\boldsymbol{\psi}}(\xi,t)\,\mathrm{d}\xi + \int_0^x \mathbf{R}(x,\xi)\tilde{\boldsymbol{\psi}}(\xi,t)\,\mathrm{d}\xi. \quad (90)$$

Denote $\tilde{\boldsymbol{\eta}} = \tilde{\boldsymbol{\psi}}_t$, $\tilde{\boldsymbol{\theta}} = \tilde{\boldsymbol{\eta}}_t$, $\tilde{\mathbf{Y}} = \dot{\tilde{\mathbf{X}}}$, and $\tilde{\mathbf{Z}} = \dot{\tilde{\mathbf{Y}}}$. Taking a partial derivative of (85)-(88) with respect to t, we have

$$\tilde{\boldsymbol{\eta}}_t = \mathbf{\Sigma}(x)\tilde{\boldsymbol{\eta}}_x + \mathbf{G}_2[\tilde{\boldsymbol{\psi}},\tilde{\boldsymbol{\eta}},\tilde{\mathbf{X}},\tilde{\mathbf{Y}}] \quad (91)$$

$$\tilde{\eta}_1(0,t) = q\tilde{\eta}_2(0,t) \quad (92)$$

$$\tilde{\eta}_2(1,t) = 0 \quad (93)$$

$$\dot{\tilde{\mathbf{Y}}}(t) = e^{\mathbf{A}d}\left(\mathbf{A}-\mathbf{LC}\right)e^{-\mathbf{A}d}\tilde{\mathbf{Y}}(t) - e^{\mathbf{A}d}\mathbf{L}\tilde{\eta}_1(1,t). \quad (94)$$

where

$$\begin{aligned}&\mathbf{G}_2[\tilde{\boldsymbol{\psi}},\tilde{\boldsymbol{\eta}},\tilde{\mathbf{X}},\tilde{\mathbf{Y}}]\\ &= \mathcal{P}\left[\frac{\partial \mathbf{f}}{\partial \tilde{\boldsymbol{\psi}}}\left(\mathcal{O}[\tilde{\boldsymbol{\psi}}],\tilde{\mathbf{X}}\right)\mathcal{O}[\tilde{\boldsymbol{\eta}}] + \frac{\partial \mathbf{f}}{\partial \tilde{\mathbf{X}}}\left(\mathcal{O}[\tilde{\boldsymbol{\psi}}],\tilde{\mathbf{X}}\right)\tilde{\mathbf{Y}}\right.\\ &\quad \left. - \frac{\partial \mathbf{f}}{\partial \tilde{\boldsymbol{\psi}}}\left(\mathcal{R}[\tilde{\boldsymbol{\psi}}],\tilde{\mathbf{X}}\right)\mathcal{R}[\tilde{\boldsymbol{\eta}}] - \frac{\partial \mathbf{f}}{\partial \tilde{\mathbf{X}}}\left(\mathcal{R}[\tilde{\boldsymbol{\psi}}],\tilde{\mathbf{X}}\right)\tilde{\mathbf{Y}}\right]. \end{aligned} \quad (95)$$

Furthermore, taking a partial derivative of (91)-(94) with respect to t, we have

$$\tilde{\boldsymbol{\theta}}_t = \mathbf{\Sigma}(x)\tilde{\boldsymbol{\theta}}_x + \mathbf{G}_3[\tilde{\boldsymbol{\psi}},\tilde{\boldsymbol{\eta}},\tilde{\boldsymbol{\theta}},\tilde{\mathbf{X}},\tilde{\mathbf{Y}},\tilde{\mathbf{Z}}] \quad (96)$$

$$\tilde{\theta}_1(0,t) = q\tilde{\theta}_2(0,t) \quad (97)$$

$$\tilde{\theta}_2(1,t) = 0 \quad (98)$$

$$\dot{\tilde{\mathbf{Z}}}(t) = e^{\mathbf{A}d}\left(\mathbf{A}-\mathbf{LC}\right)e^{-\mathbf{A}d}\tilde{\mathbf{Z}}(t) - e^{\mathbf{A}d}\mathbf{L}\tilde{\theta}_1(1,t). \quad (99)$$

where

$$\begin{aligned}
&\mathbf{G}_3[\tilde{\boldsymbol{\psi}},\tilde{\boldsymbol{\eta}},\tilde{\boldsymbol{\theta}},\tilde{\mathbf{X}},\tilde{\mathbf{Y}},\tilde{\mathbf{Z}}]\\
&=\mathcal{P}\left[\left(\frac{\partial^2\mathbf{f}}{\partial\tilde{\boldsymbol{\psi}}^2}\otimes\mathcal{O}[\tilde{\boldsymbol{\eta}}]\right)\mathcal{O}[\tilde{\boldsymbol{\eta}}]+\frac{\partial\mathbf{f}}{\partial\tilde{\boldsymbol{\psi}}}\left(\mathcal{O}[\tilde{\boldsymbol{\psi}}],\tilde{\mathbf{X}}\right)\mathcal{O}[\tilde{\boldsymbol{\theta}}]\right.\\
&\quad+\left(\frac{\partial^2\mathbf{f}}{\partial\tilde{\mathbf{X}}^2}\otimes\tilde{\mathbf{Y}}\right)\tilde{\mathbf{Y}}+\frac{\partial\mathbf{f}}{\partial\tilde{\mathbf{X}}}\left(\mathcal{O}[\tilde{\boldsymbol{\psi}}],\tilde{\mathbf{X}}\right)\tilde{\mathbf{Z}}\\
&\quad-\left(\frac{\partial^2\mathbf{f}}{\partial\tilde{\boldsymbol{\psi}}^2}\otimes\mathcal{R}[\tilde{\boldsymbol{\eta}}]\right)\mathcal{R}[\tilde{\boldsymbol{\eta}}]-\frac{\partial\mathbf{f}}{\partial\tilde{\boldsymbol{\psi}}}\left(\mathcal{R}[\tilde{\boldsymbol{\psi}}],\tilde{\mathbf{X}}\right)\mathcal{R}[\tilde{\boldsymbol{\theta}}]\\
&\quad\left.-\left(\frac{\partial^2\mathbf{f}}{\partial\tilde{\mathbf{X}}^2}\otimes\tilde{\mathbf{Y}}\right)\tilde{\mathbf{Y}}-\frac{\partial\mathbf{f}}{\partial\tilde{\mathbf{X}}}\left(\mathcal{R}[\tilde{\boldsymbol{\psi}}],\tilde{\mathbf{X}}\right)\tilde{\mathbf{Z}}\right]. \qquad (100)
\end{aligned}$$

Here, $\left(\frac{\partial^2\mathbf{f}}{\partial\tilde{\boldsymbol{\psi}}^2}\otimes\mathcal{O}[\tilde{\boldsymbol{\eta}}]\right)$ denotes a Kronecker-like product of a third order tensor of Hessian matrices $\frac{\partial^2\mathbf{f}}{\partial\tilde{\boldsymbol{\psi}}^2}=\begin{pmatrix}\mathbf{H}(\mathbf{f}_1)\\ \mathbf{H}(\mathbf{f}_2)\end{pmatrix}$ with the vector $\mathcal{O}[\tilde{\boldsymbol{\eta}}]$ and is defined as $\frac{\partial^2\mathbf{f}}{\partial\tilde{\boldsymbol{\psi}}^2}\otimes\mathcal{O}[\tilde{\boldsymbol{\eta}}]=(\mathbf{H}(\mathbf{f}_1)\mathcal{O}[\tilde{\boldsymbol{\eta}}]\quad\mathbf{H}(\mathbf{f}_2)\mathcal{O}[\tilde{\boldsymbol{\eta}}])^\intercal$. The extended ODE observer states (88), (94), (99) are useful when proving the stability of the error system (85)-(88) in the $\mathbb{H}^2$ norm through the following sequence of lemmas.

Lemma 5 *Let*

$$\begin{aligned}
V_1(t)&=\tilde{\mathbf{X}}(t)^\intercal e^{-\mathbf{A}^\intercal d}\mathbf{S}e^{-\mathbf{A}d}\tilde{\mathbf{X}}(t)\\
&\quad+\int_0^1\tilde{\boldsymbol{\psi}}^\intercal(x,t)\mathbf{D}(x)\tilde{\boldsymbol{\psi}}(x,t)\,\mathrm{d}x. \qquad (101)
\end{aligned}$$

There exists δ_1 such that if $\|\tilde{\boldsymbol{\psi}}\|_\infty<\delta_1$, then

$$\begin{aligned}
\dot{V}_1&\le-\bar{\lambda}_1V_1-\bar{\lambda}_2\left(\tilde{\psi}_1(1,t)^2+\tilde{\psi}_2(0,t)^2\right)+C_1V_1^{3/2}\\
&\quad+C_2\|\tilde{\boldsymbol{\psi}}_x\|_\infty V_1 \qquad (102)
\end{aligned}$$

where $\bar{\lambda}_1$, $\bar{\lambda}_2$, C_1 and C_2 are positive constants.

Proof *Computing the first derivative of* (101) *along* (85)-(88) *with respect to t, we have:*

$$\begin{aligned}
\dot{V}_1(t)&=\tilde{\mathbf{X}}^\intercal e^{-\mathbf{A}^\intercal d}\left((\mathbf{A}-\mathbf{LC})^\intercal\mathbf{S}+\mathbf{S}(\mathbf{A}-\mathbf{LC})\right)\\
&\quad\times e^{-\mathbf{A}d}\tilde{\mathbf{X}}-2\tilde{\mathbf{X}}^\intercal e^{-\mathbf{A}^\intercal d}\mathbf{SL}\tilde{\psi}_1(1,t)\\
&\quad+\left[\tilde{\boldsymbol{\psi}}^\intercal(x,t)\mathbf{D}(x)\boldsymbol{\Sigma}(x)\tilde{\boldsymbol{\psi}}(x,t)\right]_0^1\\
&\quad-\int_0^1\tilde{\boldsymbol{\psi}}^\intercal(x,t)\left(\mathbf{D}(x)\boldsymbol{\Sigma}(x)\right)_x\tilde{\boldsymbol{\psi}}(x,t)\,\mathrm{d}x\\
&\quad+2\int_0^1\tilde{\boldsymbol{\psi}}^\intercal(x,t)\mathbf{D}(x)\mathbf{G}_1[\tilde{\boldsymbol{\psi}},\tilde{\mathbf{X}}]\,\mathrm{d}x. \qquad (103)
\end{aligned}$$

The second term of the right hand side of (103) *can be estimated as*

$$|2\tilde{\mathbf{X}}^\intercal e^{-\mathbf{A}^\intercal d}\mathbf{SL}\tilde{\psi}_1(1,t)|\le K_0\left(|\tilde{\mathbf{X}}|^2+\tilde{\psi}_1(1,t)^2\right) \qquad (104)$$

while the last terms can be estimated as

$$2\int_0^1\tilde{\boldsymbol{\psi}}^\intercal\mathbf{D}(x)\mathbf{G}_1[\tilde{\boldsymbol{\psi}},\tilde{\mathbf{X}}]\,\mathrm{d}x\le K_1\int_0^1|\tilde{\boldsymbol{\psi}}||\mathbf{G}_1[\tilde{\boldsymbol{\psi}},\tilde{\mathbf{X}}]|\,\mathrm{d}x \qquad (105)$$

From (49) *and* (84), *for $\|\tilde{\boldsymbol{\psi}}\|_\infty\le\delta_1$, we have*

$$\int_0^1|\tilde{\boldsymbol{\psi}}||\mathbf{G}_1[\tilde{\boldsymbol{\psi}},\tilde{\mathbf{X}}]|\,\mathrm{d}x\le K_2\|\tilde{\boldsymbol{\psi}}\|_\infty\left(|\tilde{\mathbf{X}}|^2+\|\tilde{\boldsymbol{\psi}}\|_{\mathbb{L}^2}^2\right). \qquad (106)$$

Since $|\tilde{\mathbf{X}}|^2+\|\tilde{\boldsymbol{\psi}}\|_{\mathbb{L}^2}^2\le K_3V_1$ and using (12) *we have*

$$\int_0^1|\tilde{\boldsymbol{\psi}}||\mathbf{G}_1[\tilde{\boldsymbol{\psi}},\tilde{\mathbf{X}}]|\,\mathrm{d}x\le K_4\|\tilde{\boldsymbol{\psi}}_x\|_\infty V_1+K_5V_1^{3/2}. \qquad (107)$$

Substituting (104), *and* (107) *into* (103) *conclude the proof.*

Lemma 6 *Let*

$$\begin{aligned}
V_2(t)&=V_1(t)+\tilde{\mathbf{Y}}(t)^\intercal e^{-\mathbf{A}^\intercal d}\mathbf{S}e^{-\mathbf{A}d}\tilde{\mathbf{Y}}(t)\\
&\quad+\int_0^1\tilde{\boldsymbol{\eta}}^\intercal(x,t)\mathbf{D}(x)\tilde{\boldsymbol{\eta}}(x,t)\,\mathrm{d}x. \qquad (108)
\end{aligned}$$

There exists δ_2 such that if $\|\tilde{\boldsymbol{\psi}}\|_\infty<\delta_2$, then

$$\begin{aligned}
\dot{V}_2&\le-\bar{\lambda}_3V_2-\bar{\lambda}_2\left(\tilde{\psi}_1(1,t)^2+\tilde{\psi}_2(0,t)^2\right)\\
&\quad-\bar{\lambda}_4\left(\tilde{\eta}_1(1,t)^2+\tilde{\eta}_2(0,t)^2\right)+C_1V_1^{3/2}\\
&\quad+C_2\|\tilde{\boldsymbol{\psi}}_x\|_\infty V_1+C_3V_2^{3/2}+C_4\|\tilde{\boldsymbol{\eta}}_x\|_\infty V_2 \qquad (109)
\end{aligned}$$

where $\bar{\lambda}_3$, $\bar{\lambda}_4$, C_3, and C_4 are positive constants.

Proof *Computing the first derivative of* (108) *along* (91)-(94) *with respect to t, yields*

$$\begin{aligned}
\dot{V}_2(t)&=\dot{V}_1(t)\\
&\quad+\tilde{\mathbf{Y}}^\intercal e^{-\mathbf{A}^\intercal d}\left((\mathbf{A}-\mathbf{LC})^\intercal\mathbf{S}+\mathbf{S}(\mathbf{A}-\mathbf{LC})\right)\\
&\quad\times e^{-\mathbf{A}d}\tilde{\mathbf{Y}}-2\tilde{\mathbf{Y}}^\intercal e^{-\mathbf{A}^\intercal d}\mathbf{SL}\tilde{\eta}_1(1,t)\\
&\quad+\left[\tilde{\boldsymbol{\eta}}^\intercal(x,t)\mathbf{D}(x)\boldsymbol{\Sigma}(x)\tilde{\boldsymbol{\eta}}(x,t)\right]_0^1\\
&\quad-\int_0^1\tilde{\boldsymbol{\eta}}^\intercal(x,t)\left(\mathbf{D}(x)\boldsymbol{\Sigma}(x)\right)_x\tilde{\boldsymbol{\eta}}(x,t)\,\mathrm{d}x\\
&\quad+2\int_0^1\tilde{\boldsymbol{\eta}}^\intercal(x,t)\mathbf{D}(x)\mathbf{G}_2[\tilde{\boldsymbol{\psi}},\tilde{\boldsymbol{\eta}},\tilde{\mathbf{X}},\tilde{\mathbf{Y}}]\,\mathrm{d}x. \qquad (110)
\end{aligned}$$

With the help of Lemma B.6 in [3], the last term can be estimated as

$$\begin{aligned}
&2\int_0^1\tilde{\boldsymbol{\eta}}^\intercal\mathbf{D}(x)\mathbf{G}_2[\tilde{\boldsymbol{\psi}},\tilde{\boldsymbol{\eta}},\tilde{\mathbf{X}},\tilde{\mathbf{Y}}]\,\mathrm{d}x\\
&\le K_6\int_0^1|\tilde{\boldsymbol{\eta}}||\mathbf{G}_2[\tilde{\boldsymbol{\psi}},\tilde{\boldsymbol{\eta}},\tilde{\mathbf{X}},\tilde{\mathbf{Y}}]|\,\mathrm{d}x\\
&\le K_7\|\tilde{\boldsymbol{\eta}}\|_\infty\left(|\tilde{\mathbf{X}}|^2+|\tilde{\mathbf{Y}}|^2+\|\tilde{\boldsymbol{\psi}}\|_{\mathbb{L}^2}^2+\|\tilde{\boldsymbol{\eta}}\|_{\mathbb{L}^2}^2\right) \qquad (111)
\end{aligned}$$

Following the steps as in Lemma 4, concludes the proof.

Lemma 7 *Let*

$$V_3(t) = V_2(t) + \tilde{\mathbf{Z}}(t)^\intercal e^{-\mathbf{A}^\intercal d}\mathbf{S}e^{-\mathbf{A}d}\tilde{\mathbf{Z}}(t) + \int_0^1 \tilde{\boldsymbol{\theta}}^\intercal(x,t)\mathbf{D}(x)\tilde{\boldsymbol{\theta}}(x,t)\,\mathrm{d}x. \tag{112}$$

There exists δ_3 such that if $\|\tilde{\boldsymbol{\psi}}\|_\infty + \|\tilde{\boldsymbol{\eta}}\|_\infty < \delta_3$, then

$$\begin{aligned}\dot{V}_3 \le & -\bar{\lambda}_5 V_3 - \bar{\lambda}_2\left(\tilde{\psi}_1(1,t)^2 + \tilde{\psi}_2(0,t)^2\right)\\ & -\bar{\lambda}_4\left(\tilde{\eta}_1(1,t)^2 + \tilde{\eta}_2(0,t)^2\right)\\ & -\bar{\lambda}_6\left(\tilde{\theta}_1(1,t)^2 + \tilde{\theta}_2(0,t)^2\right) + C_1 V_1^{3/2}\\ & +C_2\|\tilde{\boldsymbol{\psi}}_x\|_\infty V_1 + C_3 V_2^{3/2} + C_4\|\tilde{\boldsymbol{\eta}}_x\|_\infty V_2\\ & +C_5\|\tilde{\boldsymbol{\psi}}\|_\infty V_3 + C_6\|\tilde{\boldsymbol{\eta}}\|_\infty V_3\end{aligned} \tag{113}$$

where $\bar{\lambda}_5$, $\bar{\lambda}_6$, C_5, and C_6 are positive constants.

Proof *Computing the first derivative of* (112) *along* (96)-(99) *with respect to t, yields*

$$\begin{aligned}\dot{V}_3(t) = & \dot{V}_2(t)\\ & +\tilde{\mathbf{Z}}^\intercal e^{-\mathbf{A}^\intercal d}\left((\mathbf{A}-\mathbf{LC})^\intercal\mathbf{S} + \mathbf{S}(\mathbf{A}-\mathbf{LC})\right)\\ & \times e^{-\mathbf{A}d}\tilde{\mathbf{Z}} - 2\tilde{\mathbf{Z}}^\intercal e^{-\mathbf{A}^\intercal d}\mathbf{S}\mathbf{L}\tilde{\theta}_1(1,t)\\ & +\left[\tilde{\boldsymbol{\theta}}^\intercal(x,t)\mathbf{D}(x)\boldsymbol{\Sigma}(x)\tilde{\boldsymbol{\theta}}(x,t)\right]_0^1\\ & -\int_0^1 \tilde{\boldsymbol{\theta}}^\intercal(x,t)\left(\mathbf{D}(x)\boldsymbol{\Sigma}(x)\right)_x\tilde{\boldsymbol{\theta}}(x,t)\,\mathrm{d}x\\ & +2\int_0^1 \tilde{\boldsymbol{\theta}}^\intercal\mathbf{D}(x)\mathbf{G}_3[\tilde{\boldsymbol{\psi}},\tilde{\boldsymbol{\eta}},\tilde{\boldsymbol{\theta}},\tilde{\mathbf{X}},\tilde{\mathbf{Y}},\tilde{\mathbf{Z}}]\,\mathrm{d}x.\end{aligned} \tag{114}$$

With the help of Lemma B.8 in [3], the last term can be estimated as

$$\begin{aligned}& 2\int_0^1 \tilde{\boldsymbol{\theta}}^\intercal\mathbf{D}(x)\mathbf{G}_3[\tilde{\boldsymbol{\psi}},\tilde{\boldsymbol{\eta}},\tilde{\boldsymbol{\theta}},\tilde{\mathbf{X}},\tilde{\mathbf{Y}},\tilde{\mathbf{Z}}]\,\mathrm{d}x \qquad (115)\\ & \le K_8\int_0^1 |\tilde{\boldsymbol{\theta}}||\mathbf{G}_3[\tilde{\boldsymbol{\psi}},\tilde{\boldsymbol{\eta}},\tilde{\boldsymbol{\theta}},\tilde{\mathbf{X}},\tilde{\mathbf{Y}},\tilde{\mathbf{Z}}]|\,\mathrm{d}x\\ & \le K_9\left(\|\tilde{\boldsymbol{\psi}}\|_\infty + \|\tilde{\boldsymbol{\eta}}\|_\infty\right)\\ & \times\left(|\tilde{\mathbf{X}}|^2 + |\tilde{\mathbf{Y}}|^2 + |\tilde{\mathbf{Z}}|^2 + \|\tilde{\boldsymbol{\psi}}\|_{\mathbb{L}^2}^2 + \|\tilde{\boldsymbol{\eta}}\|_{\mathbb{L}^2}^2 + \|\tilde{\boldsymbol{\theta}}\|_{\mathbb{L}^2}^2\right).\end{aligned}$$

This concludes the proof.

Remark that, a necessary condition for (85)-(88) to be well-posed in the space $\mathbb{H}^2$ is that the initial conditions verify the corresponding second-order compatibility conditions as follow [3]:

$$q_0^\intercal\tilde{\boldsymbol{\psi}}_0(0) = 0 \tag{116}$$

$$q_1^\intercal\tilde{\boldsymbol{\psi}}_0(1) = 0 \tag{117}$$

$$q_0^\intercal\left(\boldsymbol{\Sigma}(0)\tilde{\boldsymbol{\psi}}_{x0}(0) + \mathbf{G}_1[\tilde{\boldsymbol{\psi}}_0(0),\tilde{\mathbf{X}}(0)]\right) = 0 \tag{118}$$

$$q_1^\intercal\left(\boldsymbol{\Sigma}(1)\tilde{\boldsymbol{\psi}}_{x0}(1) + \mathbf{G}_1[\tilde{\boldsymbol{\psi}}_0(1),\tilde{\mathbf{X}}(0)]\right) = 0 \tag{119}$$

$$\begin{aligned}\dot{\tilde{\mathbf{X}}}(0) - e^{\mathbf{A}d}(\mathbf{A}-\mathbf{LC})e^{-\mathbf{A}d}\tilde{\mathbf{X}}(0)\\ +e^{\mathbf{A}d}\mathbf{L}q_2^\intercal\tilde{\boldsymbol{\psi}}_0(1) = 0,\end{aligned} \tag{120}$$

where

$$q_0^\intercal = [1 \quad -q] \quad q_1^\intercal = [0 \;\; 1] \quad q_2^\intercal = [1 \;\; 0]. \tag{121}$$

Utilizing Lemma 4, 5, 6, and 7, the main result for observer design of the semilinear PDE-ODE cascade systems can be stated as follow.

Theorem 2 *Let the components of $\mathbf{p}(x)$ be given by* (32)-(33) *and choose $\mathbf{L}$ such that $(\mathbf{A}-\mathbf{LC})$ is Hurwitz stable. Then, under assumption 5, for sufficiently small initial condition $\tilde{\mathbf{w}}_0 \in \mathbb{H}^2([0,1])$, there exists δ such that, if $\|\tilde{\mathbf{w}}_0\|_{\mathbb{H}^2} < \delta$ and if, under the transformations* (22), (49), (75), *and* (76), *the compatibility conditions* (116)-(120) *are verified, the error systems* (71)-(74) *is exponentially stable in the following norm:*

$$\left|\tilde{\mathbf{X}}(t)\right|^2 + \left|\dot{\tilde{\mathbf{X}}}(t)\right|^2 + \left|\ddot{\tilde{\mathbf{X}}}(t)\right|^2 + \|\tilde{\mathbf{w}}(\cdot,t)\|_{\mathbb{H}^2}^2. \tag{122}$$

Proof *From Lemma 6, since $V_1(t) \le V_2(t) \le V_3(t)$, we have*

$$\dot{V}_3 \le -\bar{\lambda}_5 V_3 + C_7 V_3^{3/2}. \tag{123}$$

Further, since $\|\tilde{\boldsymbol{\psi}}\|_\infty + \|\tilde{\boldsymbol{\eta}}\|_\infty \le C_8 V_3(t)$, then for sufficiently small $V_3(0)$, we have $V_3(t) \to 0$ exponentially. Since $V_3(t)$ is equivalent to the $\mathbb{H}^2$ norm of $\tilde{\boldsymbol{\psi}}$ when $\|\tilde{\boldsymbol{\psi}}\|_\infty + \|\tilde{\boldsymbol{\eta}}\|_\infty$ is sufficiently small (see [3]), there exists $\delta > 0$ and c, such that if $\|\tilde{\boldsymbol{\psi}}_0\|_{\mathbb{H}^2} \le \delta$, then

$$\begin{aligned}& |\tilde{\mathbf{X}}(t)| + \left|\dot{\tilde{\mathbf{X}}}(t)\right| + \left|\ddot{\tilde{\mathbf{X}}}(t)\right| + \|\tilde{\boldsymbol{\psi}}\|_{\mathbb{H}^2}^2 \le\\ & ce^{-\lambda}\left(|\tilde{\mathbf{X}}(0)| + \left|\dot{\tilde{\mathbf{X}}}(0)\right| + \left|\ddot{\tilde{\mathbf{X}}}(0)\right| + \|\tilde{\boldsymbol{\psi}}_0\|_{\mathbb{H}^2}^2\right).\end{aligned} \tag{124}$$

This concludes the proof.

3.3 Numerical Example

In this section, we present a numerical example to show the observer converges to the actual values. Let $\epsilon_1(x) = \epsilon_2(x) = \epsilon = 1$, $\omega_1(x) = \omega_2(x) = \omega = 0.001$, $q = 1$, and

$$\mathbf{A} = \begin{pmatrix} 0 & -\frac{2\pi}{6} \\ \frac{2\pi}{6} & 0 \end{pmatrix} \quad \text{and} \quad \mathbf{C} = \begin{pmatrix} 0 & 1 \end{pmatrix}. \tag{125}$$

The gain matrix is chosen as $\mathbf{L} = [0\ 4]^\intercal$, so that the matrix $\mathbf{A} - \mathbf{LC}$ has two negative eigenvalues, -0.2961 and -3.7039. Thus, $\mathbf{A} - \mathbf{LC}$ is Hurwitz stable. Since $\epsilon = 1$, we have $d = 1$. To compute the gains $p_1(x)$ and $p_2(x)$, we need to solve the system

$$\epsilon P^{uu}_x(x,\xi) + \epsilon P^{uu}_\xi(x,\xi) = \omega P^{vu}(x,\xi) \tag{126}$$
$$\epsilon P^{vu}_x(x,\xi) - \epsilon P^{vu}_\xi(x,\xi) = -\omega P^{uu}(x,\xi) \tag{127}$$

with boundary conditions

$$P^{uu}(0,\xi) = P^{vu}(0,\xi) \tag{128}$$
$$P^{vu}(x,x) = -\frac{\omega}{2\epsilon}. \tag{129}$$

Utilizing the result in [24], the solutions for (126)-(129) are given by:

$$P^{vu}(x,\xi) = -\frac{1}{2\epsilon}\left\{\omega I_0\left[\frac{|\omega|}{\epsilon}\sqrt{\xi^2 - x^2}\right] - |\omega|\sqrt{\frac{\xi - x}{\xi + x}} I_1\left[\frac{|\omega|}{\epsilon}\sqrt{\xi^2 - x^2}\right]\right\} \tag{130}$$

$$P^{uu}(x,\xi) = \frac{1}{2\epsilon}\left\{\omega I_0\left[\frac{|\omega|}{\epsilon}\sqrt{\xi^2 - x^2}\right] - |\omega|\sqrt{\frac{\xi + x}{\xi - x}} I_1\left[\frac{|\omega|}{\epsilon}\sqrt{\xi^2 - x^2}\right]\right\} \tag{131}$$

where I_n denotes the modified Bessel function of the first kind. Substituting these solutions into (32) and (33), we obtain explicit expressions for $p_1(x)$ and $p_2(x)$, respectively. Simulating the error system (71)-(74), using the above data, the error variables converge to zero as can be seen in **Fig** 1.

4 Application in Oil Well Drilling

4.1 Drilling Process

The present paper is motivated by process monitoring-problems in oil well drilling. A hydraulic well model used for annular flow and pressure estimations can be transformed into (1)-(4). To illustrate the problem, consider a simple drilling system in **Fig**. 2.

During drilling, mud from the mud pit is pumped down through the drill string, through the drill bit, up the annulus, and back to the mud pit. The objectives are to ascertain the downhole-pressure-environment limits, manage the annular hydraulic pressure profile accordingly, and to clean the well from cuttings [34]. The drill bit pressure operates between two pressure limits, namely pore pressure and fracture pressure. If the drill bit pressure goes below the pore pressure, the formation fluid start to flow into the wellbore and up the annulus. This

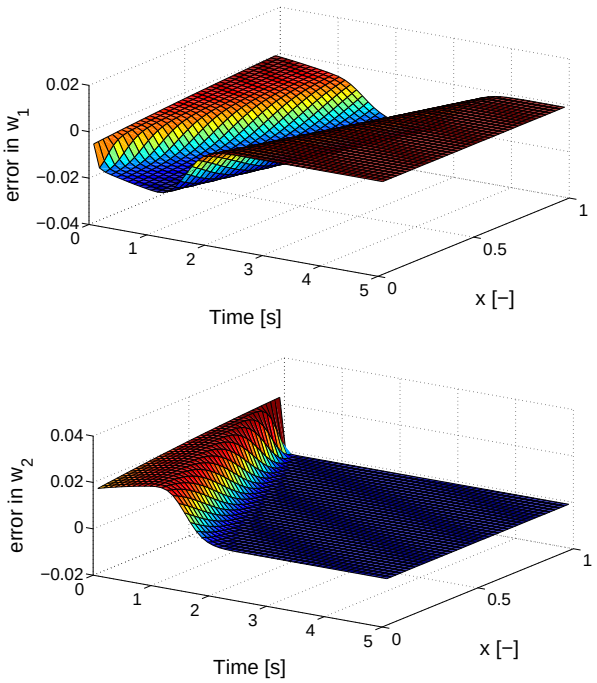

Fig. 1. Estimation errors $\tilde{w}_1(x,t)$ and $\tilde{w}_2(x,t)$.

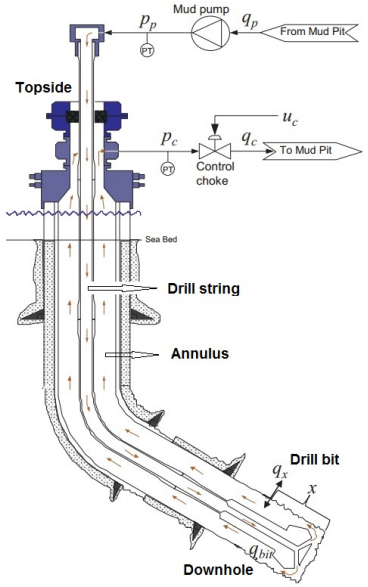

Fig. 2. Schematics of an oil well drilling (Courtesy of Statoil).

situation is called kick. In the other hand, if the drill bit pressure is close to the fracture pressure, a significant amount of mud will go into the formation, causing loss of the pressure barrier (which in turn may cause a kick). The implication of such undesirable conditions are not only economical, but also environmental and concerns worker's safety [35]. Therefore, process monitoring in oil well drilling is very crucial. Furthermore, when drilling in deep-water formation from a floating rig (a

semi-submersible rig or a drill ship), the problem is even more complicated. The wave-induced heaving motion of the drilling rig can cause a major pressure variation over the drill bit [36]. The pressure variation sometimes causes undesirable interruptions in the operation with large delay in the drilling schedule.

The dynamics inside the drill string and inside the annulus can be modeled by a hydraulic well model which can be transformed into (1)-(3), while kicks, losses, and heaving motion can be modeled by (4). A challenge in oil well drilling is that the only reliable measurement is located at the top of the well. Thus, for monitoring process, there is an incentive to estimate the system state (flow and pressure) and the system parameter (the rate of kick or the rate of lost circulation) using only a topside measurement ($x = 1$). We consider a real estimation problem in oil well drilling. The task is to monitor pressure and flow inside the annulus using only topside measurement. The challenge is that the downhole boundary parameter is uncertain due to lost circulation. Thus, we are dealing with an adaptive observer problem.

4.2 Detecting Lost Circulation

As mentioned, if the downhole pressure becomes too high, mud flows into the geological formation causing lost circulation. Lost circulation is considered to be the biggest contributor to non-productive time (NPT) in drilling operations. Depending on how many barrels are lost to the formation, the lost circulation can be categorized as seepage, typically less than 10 bbl/h; partial, typically greater than 10 bbl/h but some fluid returns; and total, no-fluid comes out of the annulus [37,38]. Total lost circulation can result in a catastrophic loss of well control. Even in the two less severe forms, lost circulation represents a financial loss that must be dealt with by the industry, the impact of which is directly tied to the per-barrel cost of the drilling fluid and the loss rate over time. Because the rate of lost circulation is unknown, in earlier drilling-process monitoring systems, e.g., [30], this quantity, which is defined as the boundary parameter of the hydraulic model, is assumed equal to the rate from the mud pump. Thus, the accuracy of the estimates is poor. In the following section, we present an analytical formula to estimate this boundary parameter.

4.3 Hydraulic Well Model

A reasonable hydraulic well model for fluid flow inside the annulus during drilling is given in [39] as

$$p_t(z,t) = -\frac{\beta}{A} q_z(z,t) \tag{132}$$

$$q_t(z,t) = -\frac{A}{\rho} p_z(z,t) + F_c(q(z,t)) - Ag\sin\tau(z) \tag{133}$$

$$q(0,t) = q_\theta \tag{134}$$

$$p(l,t) = p_c(t) \tag{135}$$

where p and q denote the annular pressure and flow, respectively. The Bulk modulus is denoted by β, ρ is the drilling fluid density, and A is the area of the annulus. The boundary parameter q_θ is the unknown parameter that constitutes loss. The frictional characteristic function F_c is given by

$$F_c(q(z,t)) = -\varphi_1 q(z,t) - \varphi_2 q(z,t)^2. \tag{136}$$

If the flow velocity inside the annulus is low (Reynolds number, $Re < 2000$), then the fluid exhibits laminar flow. In contrast, if the flow velocity is high ($Re > 4000$), then the fluid exhibits turbulent flow. In [40], a laminar flow is modeled by setting $\varphi_2 = 0$.

4.4 Feasibility of Design

Using algebraic transformations, it can be shown that the hydraulic well model (132)-(135) can be transformed into (1)-(4). The hydrostatic head can be removed from the momentum equation by defining

$$\bar{p}(z,t) = p(z,t) - \rho g\left(l - \int_0^z \sin\tau(s)\,\mathrm{d}s\right). \tag{137}$$

Thus, we have

$$\bar{p}_t(z,t) = -\frac{\beta}{A} q_z(z,t) \tag{138}$$

$$q_t(z,t) = -\frac{A}{\rho}\bar{p}_z(z,t) - \varphi_1 q(z,t) - \varphi_2 q(z,t)^2 \tag{139}$$

$$q(0,t) = q_\theta \tag{140}$$

$$\bar{p}(l,t) = p_c(t) - \rho g\left(l - \int_0^l \sin\tau(s)\,\mathrm{d}s\right). \tag{141}$$

The above system can be diagonalized using the following Riemann's coordinate transformation

$$\begin{aligned}\bar{w}_1(z,t) &= \frac{1}{2}\left(q(z,t) + \frac{A}{\sqrt{\beta\rho}}\bar{p}(z,t)\right)\\ \bar{w}_2(z,t) &= \frac{1}{2}\left(q(z,t) - \frac{A}{\sqrt{\beta\rho}}\bar{p}(z,t)\right)\end{aligned} \tag{142}$$

which yields

$$\bar{w}_{1t} = -\sqrt{\frac{\beta}{\rho}}\bar{w}_{1z} - \frac{\varphi_1}{2}(\bar{w}_1 + \bar{w}_2) - \frac{\varphi_2}{2}(\bar{w}_1 + \bar{w}_2)^2 \tag{143}$$

$$\bar{w}_{2t} = \sqrt{\frac{\beta}{\rho}}\bar{w}_{2z} - \frac{\varphi_1}{2}(\bar{w}_1 + \bar{w}_2) - \frac{\varphi_2}{2}(\bar{w}_1 + \bar{w}_2)^2 \tag{144}$$

The boundary conditions are given by

$$\bar{w}_1(0,t) = -\bar{w}_2(0,t) + q_\theta \tag{145}$$

$$\bar{w}_2(l,t) = U(t). \tag{146}$$

Defining $w_1(x,t) = \bar{w}_1(xl,t)$ and $w_2(x,t) = \bar{w}_2(xl,t)$, the hydraulic well model (143)-(146) resemble the semi-linear systems (1)-(4) with

$$\epsilon_1(x) = \epsilon_2(x) = \frac{1}{l}\sqrt{\frac{\beta}{\rho}} \tag{147}$$

$$\omega_1(x) = \omega_2(x) = -\frac{\varphi_1}{2} \tag{148}$$

$$\mathbf{f}(\mathbf{w},x) = \begin{pmatrix} -\frac{\varphi_1}{2}w_1 - \frac{\varphi_2}{2}(w_1+w_2)^2 \\ -\frac{\varphi_1}{2}w_2 - \frac{\varphi_2}{2}(w_1+w_2)^2 \end{pmatrix} \tag{149}$$

$$U(t) = \frac{1}{2}q(l,t) - \frac{A}{2\sqrt{\beta\rho}}\left(p_c(t) - \rho g\left(l - \int_0^l \sin\tau(s)\,\mathrm{d}s\right)\right) \tag{150}$$

$$\mathbf{C} = 1 \tag{151}$$

$$\mathbf{A} = 0 \tag{152}$$

$$\mathbf{X} = q_\theta. \tag{153}$$

4.5 The Flow-loop Test Experiment

The experiment is carried out in a field scale flow-loop test in Stavanger, Norway by Statoil. The drilling system is modeled as a U-tube (**Fig**. 3) which consists of a main pump, 1400 meters of pipes, a downhole assembly, and topside sensors (**Fig**. 4). The downhole assembly is completed with an exit valve to simulate the lost circulation problem and a Coriolis meter to measure the lost circulation rate. The topside sensors consist of a Coriolis meter to measure the return fluid and a pressure gauge to measure the pressure.

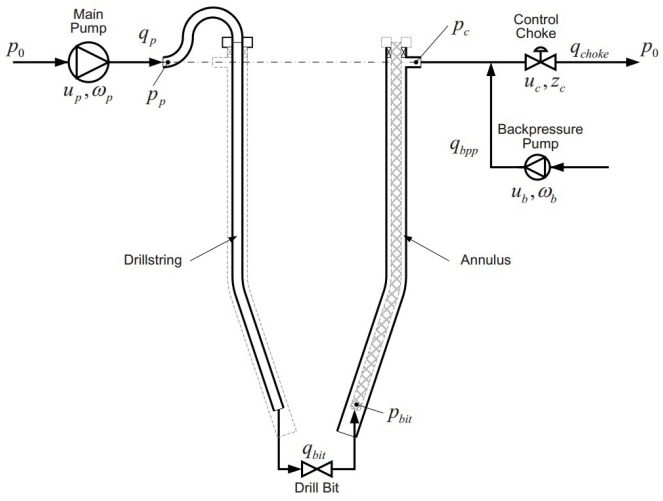

Fig. 3. Schematics of the flow-loop.

Water is injected by the main pump through the drill string and up the annulus. After some time, the downhole choke is gradually opened to simulate the lost circulation. The task is to estimate the flow and pressure along the annulus and the rate of lost circulation using only measurements at the top of the well. The topside flow and pressure measurements can be seen in **Fig**. 5. Here, the volumetric flow rate is already filtered using a robust method of local regression with weighted linear squares and 2nd-degree polynomial model. **Fig**. 6 shows the relation of the volumetric flow rate of lost circulation and the valve opening. It can be observed that the valve opening is almost linear with respect to the flow rate.

(a) Downhole assembly (b) Topside facilities

Fig. 4. The flow-loop experiment

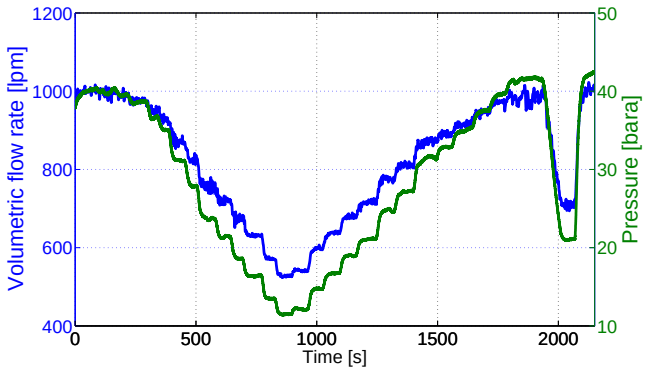

Fig. 5. Measured topside flow rate and pressure.

4.6 Simulation Results

Relying only on the topside measurement $y(t) = w_1(1,t)$, we want to estimate the downhole pressure $p(0,t)$ and the downhole flow rate under lost circulation q_θ. From the section 4.4 and based on the observer design for the semilinear systems (67)-(70), the observer for the hydraulic well model is given by

$$\hat{\mathbf{w}}_t(x,t) = \mathbf{\Sigma}\hat{\mathbf{w}}_x + \mathbf{\Omega}\hat{\mathbf{w}} + \mathbf{f}(\hat{\mathbf{w}},x) + \mathbf{p}(x)\tilde{w}_1(1,t) \tag{154}$$

$$\hat{w}_1(0,t) = -\hat{w}_2(0,t) + \hat{q}_\theta \tag{155}$$

$$\hat{w}_2(1,t) = U(t). \tag{156}$$

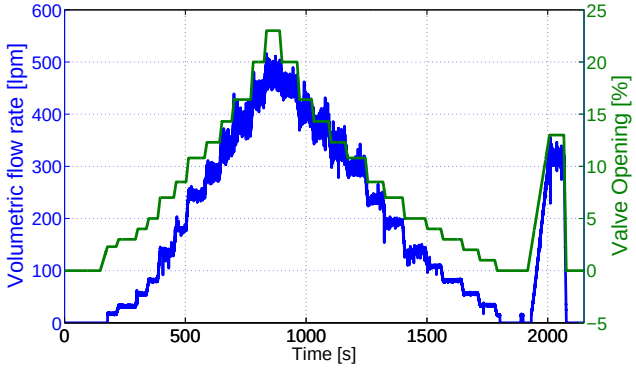

Fig. 6. Downhole exit valve opening and volumetric flow rate response.

where the downhole flow rate under lost circulation $\hat{q}_\theta$ is estimated using the update law

$$\dot{\hat{q}}_\theta(t) = \frac{\mathbf{L}}{2}\left(q_c(t) - \hat{q}_c(t) + \frac{A}{\sqrt{\beta\rho}}\left(p_c(t) - \hat{p}_c(t)\right)\right) \quad (157)$$

where q_c and p_c are measurements taken at the topside of the well. The scalar $\mathbf{L} > 0$ is the tuning parameter for the update law. Solving the observer equations (154)-(156), where the parameter q_θ is estimated using (157), the downhole pressure and the downhole flow rate under lost circulation can be accurately estimated, as shown in **Fig**. 7 and **Fig**. 8, respectively.

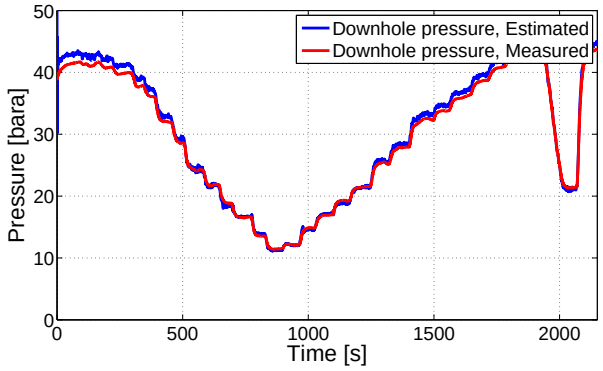

Fig. 7. Estimated and measured downhole pressure.

The estimated and measured topside pressure are in good agreement, as shown in **Fig**. 9. The deviation between $t = 800$ s and $t = 900$ s is due to the flow-loop contour, which may cause back pressure when the rate is too low. This can be improved by adjusting the geometric properties of the pipes.

5 Conclusions

We have solved the boundary observer design problem for a class of hyperbolic PDE-ODE cascade systems

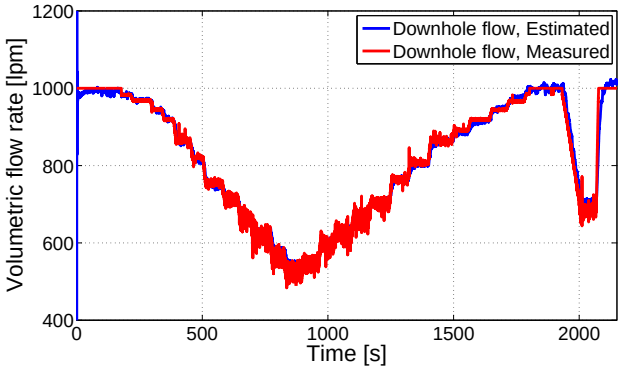

Fig. 8. Estimated and measured downhole flow rate.

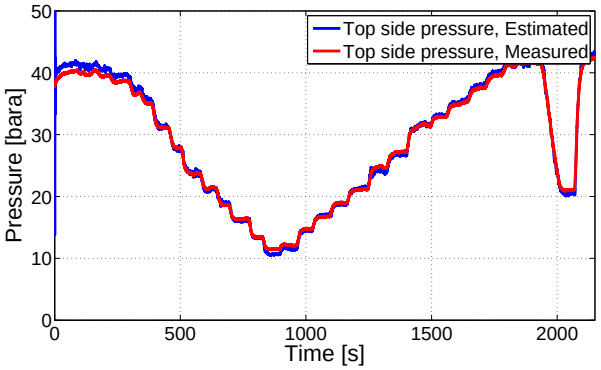

Fig. 9. Estimated and measured topside pressure.

where the sensor and actuator are located at the same boundary. The design, which is based on the backstepping method, requires only measurement at one of the boundaries. We show that the observer gain can be computed analytically by solving a first-order Goursat-type PDEs in terms of Bessel function of the first kind. The semilinear observer design is obtained from the linear design where we show the estimates converge to the actual values exponentially. A real-field process monitoring problem in oil well drilling is presented to show the usefulness of the design. Since the observer is computed almost without computational cost, the design method can be used as online process monitoring system.

It was assumed that the drilling parameters such as density and Bulk modulus of the drilling fluid is known. If these parameters are unknown, a new adaptive design should be developed. Adaptive observer for PDE-ODE cascade systems is a wide open and fertile area for future research. The presented design can also be used to predict gas kicks. In this case, a two-phase well hydraulic model may be used. A boundary observer design involving more than two PDE states may be developed for this purpose.

Acknowledgment

Financial support from Statoil ASA and the Norwegian Research Council (NFR project 210432/E30 Intelligent Drilling) is gratefully acknowledged. The experimental data are results from ongoing internal research in the department Intelligent Drilling in Statoil RDI. The authors gratefully acknowledge the work done by Alexey Pavlov, Henrik Manum and Glenn-Ole Kaasa in planning and conducting experiments.

References

[1] Vazquez, R., Coron, J.M., & Krstic, M. (2011). Backstepping boundary stabilization and state estimation of a 2×2 linear hyperbolic system. *IEEE Conference on Decision and Control*, Orlando, USA.

[2] Aamo, O.M. (2013). Disturbance rejection in 2×2 linear hyperbolic systems. *IEEE Transaction Automatic Control*, 58, 1095–1106.

[3] Coron, J.M., Vazquez, R., Krstic, M., & Bastin, G. (2013). Local exponential $\mathbb{H}^2$ stabilization of a 2×2 quasilinear hyperbolic system using backstepping. *SIAM Journal of Control and Optimization*, 51, 2005–2035.

[4] Wang, Z. (2006). Exact controllability for nonautonomous first order quasilinear hyperbolic systems. *Chinese Annals of Mathematics, Series B*, 27, 643–656.

[5] Goatin, P. (2006). The Aw-Rascle vehicular traffic flow model with phase transitions. *Mathematical and Computer Modelling*, 44, 287–303.

[6] Gugat, M., & Dick, M. (2011). Time-delayed boundary feedback stabilization of the isothermal Euler equations with friction. *Mathematical Control and Related Fields*, 1, 469–491.

[7] White, F. (2007). *Fluid Mechanics*. New York: McGraw-Hill.

[8] Hasan, A., & Imsland, L. (2014). Moving horizon estimation in managed pressure drilling using distributed models. *Proceedings of the IEEE Conference on Control Applications (CCA)*, Antibes, France.

[9] Coron, J.M., Andrea-Novel, B., & Bastin, G. (2007). A strict Lyapunov function for boundary control of hyperbolic systems of conservation laws. *IEEE Transactions on Automatic Control*, 52, 2–11.

[10] Krstic, M. (2009). Compensating actuator and sensor dynamics governed by diffusion PDEs. *Systems & Control Letters*, 58, 372–377.

[11] Susto, G.A., & Krstic, M. (2010). Control of PDE-ODE cascades with Neumann interconnections. *Journal of the Franklin Institute*, 347, 284–314.

[12] Tang S., & Xie, C. (2011). Stabilization for a coupled PDE-ODE control system. *Journal of the Franklin Institute*, 348, 2142–2155.

[13] Krstic, M., & Smyshlyaev, A. (2008). Backstepping boundary control for first-order hyperbolic PDEs and application to systems with actuator and sensor delays. *Systems & Control Letters*, 57, 750–758.

[14] Bekiaris-Liberis, N., & Krstic, M. (2011). Compensating the distributed effect of diffusion and counter-convection in multi-input and multi-output LTI systems. *IEEE Transaction Automatic Control*, 56, 637–643.

[15] Hasan, A., Krstic, M., & Aamo, O.M. (2015). State estimation for nonlinear hyperbolic PDE-ODE cascade systems. *Asian Control Conference*, Kota Kinabalu, Malaysia.

[16] Krstic, M. (2009). Compensating a string PDE in the actuation or sensing path of an unstable ODE. *IEEE Transaction Automatic Control*, 54, 1362–1368.

[17] Bekiaris-Liberis, N., & Krstic, M. (2010). Compensating the distributed effect of a wave PDE in the actuation or sensing path of MIMO LTI systems. *Systems & Control Letters*, 59, 713–719.

[18] Meurer, T. (2013). On the extended Luenbergertype observer for semilinear distributedparameter systems. *IEEE Transaction Automatic Control*, 58, 1732–1743.

[19] Jadachowski, L., Meurer, T., & Kugi, A. (2014). Backstepping observers for quasilinear parabolic pdes. *IFAC World Congress*, Capetown, South Africa.

[20] Aamo, O.M., Smyshlyaev, A., & Krstic, M. (2005). Boundary control of the linearized Ginzburg-Landau model of vortex shedding. *SIAM Journal of Control and Optimization*, 43, 1953–1971.

[21] Krstic, M., Guo, B.Z., & Smyshlyaev, A. (2011). Boundary controllers and observers for the linearized Schrodinger equation. *SIAM Journal of Control and Optimization*, 49, 1479–1497.

[22] Krstic, M., & Smyshlyaev, A. (2008). Boundary control of PDEs: a course on backstepping designs. Philadelphia: SIAM.

[23] Smyshlyaev, A., & Krstic, M. (2005). Backstepping observers for a class of parabolic PDEs. *Systems and Control Letters*, 54, 613–625.

[24] Vazquez, R., & Krstic, M. (2014). Marcum Q-functions and explicit kernels for stabilization of 2×2 linear hyperbolic systems with constant coefficients. *Systems and Control Letters*, 68, 33–42.

[25] Hasan, A., Foss, B., & Sagatun, S. (2013). Optimization of oil production under gas coning conditions. *Journal of Petroleum Science and Engineering*, 105, 26–33.

[26] Hasan, A., Sagatun, S., & Foss, B. (2010). Well rate control design for gas coning problems. *IEEE Conference on Decision and Control*, Atlanta, USA.

[27] Hasan, A., Foss, B., & Sagatun, S. (2012). Flow control of fluids through porous media. *Applied Mathematics and Computation*, 219, 3323–3335.

[28] Di Meglio, F., Vazquez, R., Krstic, M., & Petit, N. (2012). Backstepping stabilization of an underactuated 3x3 linear hyperbolic system of fluid flow equations. *American Control Conference*, Montreal, Canada.

[29] Hasan, A. (2014). Adaptive boundary control and observer of linear hyperbolic systems with application to Managed Pressure Drilling. *ASME Dynamic Systems and Control Conference*, San Antonio, USA.

[30] Hauge, E., Aamo, O.M., & Godhavn, J.M. (2013). Application of an infinite-dimensional observer for drilling systems incorporating kick and loss detection. *European Control Conference*, Zurich, Switzerland.

[31] Hasan, A. (2015). Adaptive boundary observer for nonlinear hyperbolic systems: Design and field testing in managed pressure drilling. *American Control Conference*, Chicago, USA.

[32] Hasan, A. (2014). Disturbance attenuation of $n+1$ coupled hyperbolic PDEs. *Conference on Decision and Control*, Los Angeles, USA.

[33] Anfinsen, H., & Aamo, O.M. (2015). Disturbance rejection in the interior domain of linear 2×2 hyperbolic systems. *IEEE Transaction on Automatic Control*, 60, 186–191.

[34] Hilts, B. (2013). Managed Pressure Drilling. *SPE Annual Technical Conference and Exhibition*, New Orleans, USA.

[35] Sutton, I.S. (2013). Summarizing the Deepwater horizon/Macondo reports. *Offshore Technology Conference*, Houston, USA.

[36] Nas, S.W. (2010). Deepwater Managed Pressure Drilling applications. *International Oil and Gas Conference and Exhibition*, Beijing, China.

[37] Moazzeni, A.R., Nabaei, M., & Jegarluei, S.G. (2010). Prediction of lost circulation using virtual intellegence in one of Iranian oilfields, *SPE Nigeria Annual International Conference and Exhibition*, Calabar, Nigeria.

[38] Whitfill, D.L., Wang, M., Jamison, D., & Angove-Rogers, A. (2007). Preventing lost circulation requires planning ahead. *SPE International Oil Conference and Exhibition*, Veracruz, Mexico.

[39] Landet, I.S., Pavlov, A., & Aamo, O.M. (2013). Modeling and control of heave-induced pressure fluctuations in Managed Pressure Drilling. *IEEE Transaction on Control System Technology*, 21, 1340–1351.

[40] Kaasa, G.O., Stamnes, O.N., Imsland, L., & Aamo, O.M. (2012). Simplified hydraulics model used for intelligent estimation of downhole pressure for a Managed Pressure Drilling control system. *SPE Drilling and Completion*, 27, 127–138.